• *Short report*

Acquiring molecular interference functions of X-ray coherent scattering for breast tissues by combination of simulation and experimental methods

A. Chaparian[1][*] ,M.A. Oghabian[1] , V. Changizi[2]

[1]Tehran University of Medical Sciences, Medical Physics and Biomedical Engineering Department, Tehran, Iran
[2]Tehran University of Medical Sciences, Radiology Technology Department, Tehran, Iran

Background: Recently, it has been indicated that X-ray coherent scatter from biological tissues can be used to access signature of tissue. Some scientists are interested in studying this effect to get early detection of breast cancer. Since experimental methods for optimization are time consuming and expensive, some scientists suggest using simulation. Monte Carlo (MC) codes are the best option for radiation simulation; however, one permanent defect with MC codes has been the lack of a sufficient physical model for coherent (Rayleigh) scattering, including molecular interference effects. **Materials and Methods:** It was decided to obtain molecular interference functions of coherent X-ray scattering for normal breast tissues by combination of modeling and experimental methods. A Monte Carlo simulation program was written to simulate the angular distribution of scattered photons for the normal breast tissue samples. Moreover, experimental diffraction patterns of these tissues were measured by means of energy dispersive X-ray diffraction (EDXRD) method. The simulation and experimental data were used to obtain a tabulation of molecular interference functions for breast tissues. **Results:** With this study a tabulation of molecular interference functions for normal breast tissues was prepared to facilitate the simulation diffraction patterns of the tissues without any experimental. **Conclusion:** The method may lead to design new systems for early detection of breast cancer. **Iran. J. Radiat. Res., 2009; 7 (2): 113-117**

Keywords: *X-ray coherent scattering, simulation, molecular interference functions, breast tissues.*

INTRODUCTION

Coherent X-ray scatters in the same phase may have constructive interferences which make diffraction patterns and signature of tissue. Some scientists have been interested in studying this effect to get early detection of breast cancer as it is one of the most widespread cancers among women [1].

It has been shown that coherent scattering could be used for breast tissue characterization [1-8]. All of these studies normal and cancerous breast tissue using diffraction patterns of the coherent scatters.

Hitherto most of studies have been performed on samples with long time exposure, it is necessary to optimize the system in order to be feasible for clinical usage. Since experimental methods for optimization are time consuming and expensive, simulation or modeling procedures are preferable. Monte Carlo codes are currently used for radiation simulation; however, one problem with MC codes is the lack of a satisfactory physical model for coherent (Rayleigh) scattering including molecular interference effects. Tartari *et al.* proposed that the usual tabulations of coherent scattering data performed in the frame of independent atomic modelling (IAM) had to be updated, or replaced by an appropriate customization [9]. Their study was performed using a basic set of curves for the linear differential

*Corresponding author:
Dr. Ali Chaparian,
Medical Physics and Biomedical Engineering Department, Tehran University of Medical Sciences, Keshavarz Blvd., Poursina Ave., Tehran, Iran.
Fax: +98 21 88973653
E-mail: chaparian@razi.tums.ac.ir

scattering coefficients of water, fat, and of bone tissue in terms of its mineral and nonmineral components.

Regarding to necessity of coherent system optimization for early detection of breast cancer, we are going to obtain molecular form factor and a self-consistent basic set of tabulations for normal breast tissues in terms of its adipose and glandular components.

Theoretical concepts

The differential cross section per unit solid angle for Thomson scattering from a free electron at angle θ is:

$$\frac{d_e \sigma_{T\text{ hom son}}}{d_\sigma} = \frac{r_e^2}{2}\left(1 + \cos^2 \theta\right) \qquad (1)$$

Where r_e is the classical electron radius. For elements according to wave's interference, the coherent scattering cross section per steradian is:

$$\frac{d\sigma_{coh}}{d_\sigma} = \frac{r_e^2}{2}\left(1 + \cos^2 \theta\right)F^2(\chi, Z) \qquad (2)$$

Where Z is the atomic number, and F(χ,Z) is the coherent scatter form factor for element Z and $0 \leq F(\chi,Z) \leq Z$. The momentum transfer, χ is calculated from:

$$\chi = \frac{1}{\lambda}\sin\frac{\theta}{2} = \frac{E}{hc}\sin\frac{\theta}{2} \qquad (3)$$

For complex materials, the form factor can be calculated as the Independent Atom Model (IAM),

$$F_{IAM}^2(\chi) = \sum_i n_i F^2(\chi, Z_i) \qquad (4)$$

Where n_i is the number fraction of element i. However the IAM is valid only at large *x*, since intra-atomic interference hasn't been considered [10].

Using the model proposed by Narten and Levy [10], the molecular form factor for complex materials can be calculated as:

$$F_{MOL}^2(\chi) = F_{IAM}^2(\chi).s(\chi) \qquad (5)$$

Where *s (χ)* is an oscillatory structure function which accounts for the molecular and intermolecular interference effects. For amorphous materials and liquids, *s (χ)* shows a damped behavior around unity and for high values of χ the amplitudes of the oscillations strongly decrease and $F_{MOL}^2(\chi)$ is approximated well by $F_{IAM}^2(\chi)$.

Therefore, for a tissue, the default MC items are used to form the resulting IAM squared form factor; then these data must be multiplied by the corresponding values of *s (χ)* to obtain the squared form factors.

MATERIALS AND METHODS

Obtaining of the IAM squared form factor

In order to simulate the angular distribution of scattered photons and obtain IAM squared form factor for the breast tissue samples, a Monte Carlo simulation program was written.

The MC code had taken all the relevant processes into account (photoelectric effect, coherent scattering and Compton scattering), the geometrical and physical properties of source, sample and detector. IAM squared form factor were obtained using the form factor of coherent scattering according to tables of Hubbell *et al.* [11].

Elemental composition of breast tissues:
Accurate modeling of the interactions within the tissue would require an exact knowledge of its composition. The composition of each tissue (i.e., fractional weights of each type of atom) must be known in order to calculate using $F_{IAM}^2(\chi)$ the sum rule (equation 4). Compositions and densities of samples were obtained from ICRU Report 44 [12]. These data are shown in table 1.

Geometry of simulation: The sample was put in the center of coordinates. Detector' positions were gotten by *e*quation 3 at the momentum transfer ranging from 0 to 8 nm^{-1} (According to tables of Hubbell *et al.* [11]). Finally, the scattered intensity was plotted as a function of momentum transfer distribution.

Measurement of the squared molecular form factor: The diffraction patterns or experimental squared form factors could be

obtained either by using monoenergetic pho‐ tons and scanning the various scattering angles (angular dispersive), or by using polyenergetic photons at a certain scattering angle (energy dispersive).

The experimental squared form factors for tissue samples were obtained by means of energy dispersive X‐ray diffraction (EDXRD) method, reported previously [1, 6].

In the previous work adipose, glandular, normal breast (50/50) and water samples were used, and the scattering patterns were measured at a fixed scattering angle of 6°. The tungsten target X‐ray tube was operated at 10 mA and 80 kV. To obtain a pencil beam, two collimators, made of lead with 50‐mm length and 1‐mm hole, acceptance angle approximately 1°, were used. The detection system was a planar HpGe detector with energy resolution of 450 eV at 59.7 keV. After carrying out some corrections for background counts, the shape of the incident spectrum and attenuation through the sample, then using equation (3), energy values were transformed to momentum transfer. In this study, the experimental squared form factors were obtained for momentum transfer ranging from 0 to 3.37 nm^{-1}; therefore, for momentum transfer ranging from 3.37 to 8 nm^{-1} experimental squared form factors was acquired from study of Poletti *et al.* [4].

Calculation of oscillatory structure functions for each tissue

After correcting the diffraction pattern and removing the incoherent scattering component, the corresponding squared form factor were obtained by normalizing the data to those of the IAM values in an interval of the χ variable ranging from 6 to 8 nm^{-1}. As indicated in equation 5, oscillatory structure function $s(\chi)$ could be obtained by dividing the experimental squared form factors $F_{MOL}^2(\chi)$ by the computed values of IAM squared form factor for $F_{IAM}^2(\chi)$ every momentum transfer.

RESULTS AND DISCUSSION

The squared form factor profiles: Figure 1 show the comparison between the measured scattering profile and IAM theoretical based on the atomic form factor tabulations of Hubbell *et al.* [11] in terms of squared form factor for the selected samples. All measured curves showed similar features with a sharp maximum value for intensity in a specific momentum transfer which defined tissue signature. Each curve falled in an oscillatory mode to a smooth variation associated with the IAM model.

As shown in figure 1 (a, b, d), the peak position for adipose, glandular and water are around 1.1 nm^{-1}, 1.55 nm^{-1}, 1.6 nm^{-1} respectively. Figure 1 (c) shows scattering profile of adipose and glandular mixture (50/50) that shows two peaks of 1.1 nm^{-1} and 1.55 nm^{-1} in due to the contribution of the two components (adipose and glandular) of the tissue.

Table 1. Elemental composition and density of materials and tissues (ICRU 44).

| Tissue	Elemental Composition (percentage by mass)					Specific Gravity (kg m^{-3})
	H	C	N	O	Others	
Adipose	11.4	59.8	0.7	27.8	0.1 Na, 0.1 S, 0.1 Cl	950
Glandular	10.6	33.2	3.0	52.7	0.1 Na, 0.1 P, 0.2 S, 0.1 Cl	1020
Breast (whole)- 50/50 (water/lipid)	11.5	38.7	-	49.8	-	960
Water	11.2	-	-	88.8	-	1000
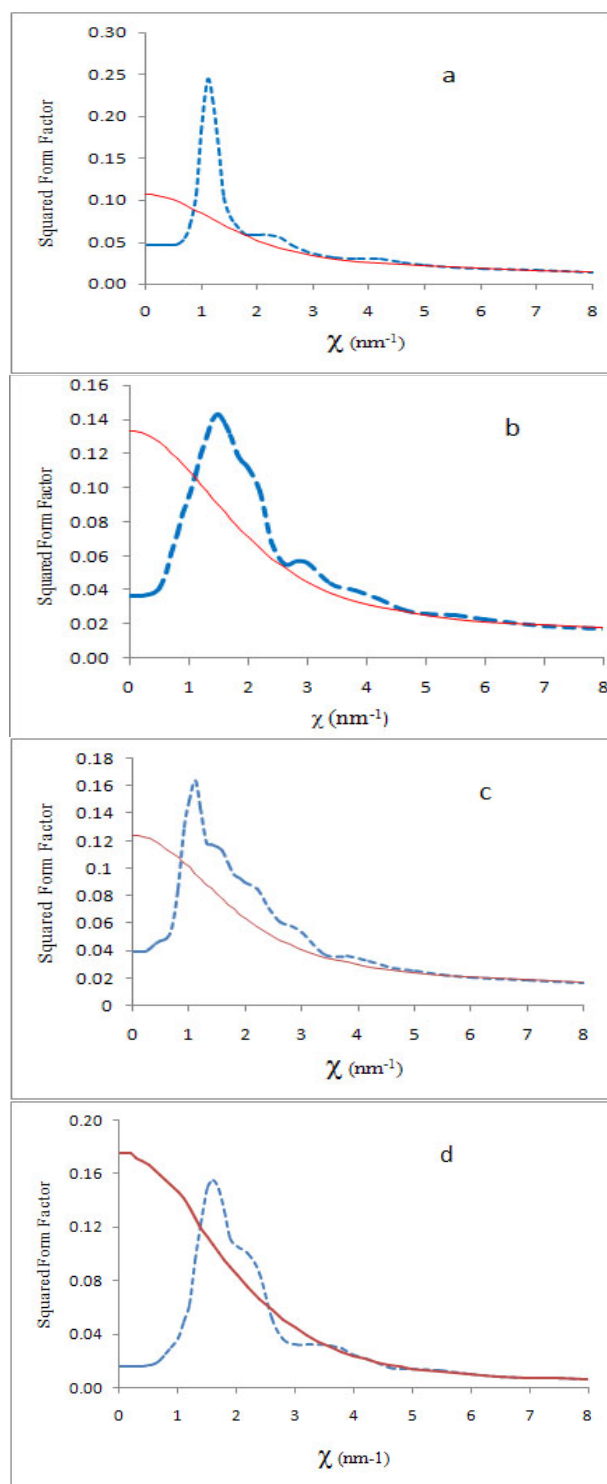
Figure 1. Measured squared form factors (—) and corresponding IAM predictions (–) for water and breast tissues: (a) adipose; (b) glandular; (c) breast (50/50); (d) water plotted with the Hubbell grid.

The oscillatory structure functions: Figure 2 shows some examples of oscillatory structure functions ($s(\chi)$) or molecular interference functions which are supplied to

integrate the tabulations of F(Z,x) used by default in the current photon transport MC codes.

The χ grids used in plotting the curves in figure 2 with intervals of 0.1 nm^{-1} have been the same as the grid which was adopted by Hubbell *et al.* [11]. Since for biological tissues, there is not an interference effect in x higher than 8 nm^{-1}, so a reduced grid version of the $s(\chi)$ functions was considered in figure 2 and the results are reported in table 2. After $\chi = 8$, the values are assumed to be equal to unity.
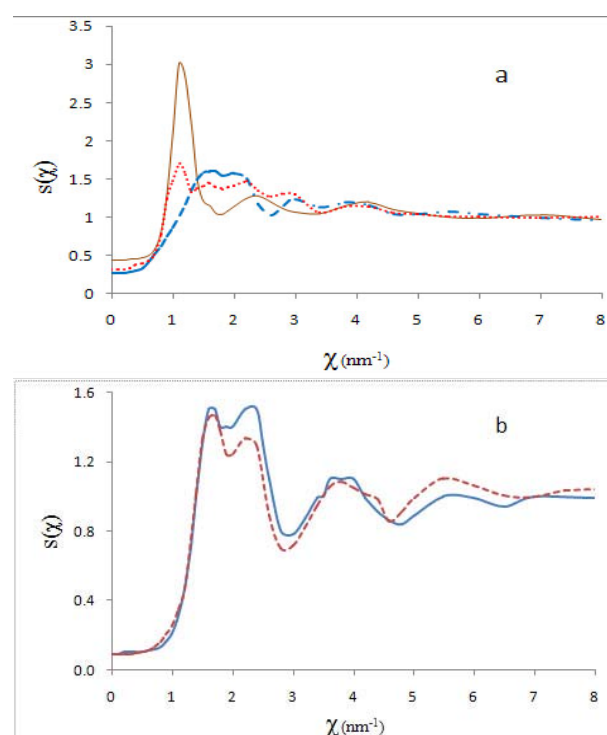
Figure 2. Plots of structure functions (a) for tissues include adipose (—), glandular (- -) and breast (50/50)(---), (b) Comparison of structure functions for water obtained in our study (---) and Tartari's study (-).

CONCLUSION

This study presented a tabulation of the oscillatory structure or molecular interference functions ($s(\chi)$) for normal breast tissues. These values can be incorporated in Monte Carlo codes to simulate diffraction patterns of these tissues.

The achieved result for oscillatory structure curve of water was the same as Tartari *et al.* [9], and it could be used for both studies validation. Although a little

Table 2. Molecular interference functions s(χ) for breast tissue components and water.

χ (nm^{-1})	Adipose Tissue	Glandular Tissue	Breast (50/50)	Water
0	0.44	0.275	0.319	0.092
0.1	0.44	0.275	0.319	0.092
0.2	0.44	0.276	0.322	0.092
0.3	0.45	0.283	0.338	0.093
0.4	0.46	0.295	0.376	0.097
0.5	0.47	0.325	0.401	0.102
0.6	0.50	0.408	0.430	0.109
0.7	0.59	0.514	0.505	0.131
0.8	0.77	0.629	0.790	0.163
0.9	1.22	0.745	1.248	0.205
1	2.16	0.867	1.481	0.253
1.1	3.01	1.023	1.697	0.349
1.2	2.87	1.173	1.555	0.463
1.3	2.17	1.341	1.331	0.751
1.4	1.47	1.494	1.379	1.020
1.5	1.21	1.594	1.419	1.330
1.6	1.14	1.601	1.450	1.449
1.7	1.05	1.597	1.400	1.463
1.8	1.04	1.546	1.371	1.383
1.9	1.08	1.556	1.393	1.242
2	1.14	1.577	1.414	1.244
2.2	1.25	1.512	1.468	1.335
2.4	1.28	1.167	1.350	1.296
2.6	1.20	1.034	1.269	0.888
2.8	1.11	1.160	1.310	0.704
3	1.07	1.239	1.300	0.719
3.4	1.05	1.137	1.065	0.820
3.8	1.14	1.192	1.144	0.946
4.2	1.20	1.161	1.141	1.055
4.6	1.10	1.048	1.056	1.082
5	1.05	1.045	1.036	1.047
5.5	1.00	1.075	1.011	1.015
6	0.99	1.048	1.001	0.980
7	1.03	0.987	0.998	0.857
8	0.97	0.956	1.001	0.909

difference was found between intensities in these two studies, it could have been due to the use of different set ups. Johns *et al.* [13] showed the same difference for five workers related to water too.

Finally, the results of this study can help to simulate scattering behavior of breast tissues and to design new systems for early detection of breast cancer. The work is still in progress to obtain elemental composition of cancerous breast tissues.

REFERENCES

1. Changizi V, Arab Kheradmand A, Oghabian MA (2008) Application of small angle x-ray scattering (SAXS) for differentiation among breast tumors. *J Med Phys, 33:19-23.*
2. Evans SH, Bradley DA, Dance DR, Bateman JE, Jones CH (1991) Measurement of small-angle photon scattering for some breast tissues and tissue substitute materials. *Phys Med Biol, 36: 7–18.*
3. Kidane G, Speller RD, Royle GJ, Hanby AM (1999) X-ray scatter signatures for normal and neoplastic breast tissues. *Phys Med Biol, 44: 1791–802.*
4. Poletti ME, Goncalves OD, Mazzaro I (2002) Coherent and incoherent scattering of 17.44 and 6.93 keV X-ray photons scattered from biological and biological-equivalent samples: characterization of tissues. *X-ray Spectrom, 31: 57–61.*
5. Ryan E and Farquharson MJ (2004) Angular dispersive X-ray scattering from breast tissue using synchrotron radiation. *Radiat Phys Chem, 71: 971–972.*
6. Changizi V, Oghabian MA, Speller RD, Sarkar S, Arab Kheradmand A (2005) Application of small angle x-ray scattering (SAXS) for differentiation between normal and cancerous breast tissue. *Int J Med Sci, 2:118–121.*
7. Cunha DM, Oliveira OR, Perez CA, Poletti ME (2006) X-ray scattering profiles of some normal and malignant human breast tissues. *X-ray Spectrom, 35: 370–374.*
8. Oliveira OR, Conceicao LC *et al.* (2008) Identification of neoplasias of breast tissues using a powder diffracto-meter. *J Radiat Res, 49: 527-532.*
9. Tartari A, Taibi A, Bonifazzi C, Baraldi C (2001) Updating of form factor tabulations for coherent scattering of photons in tissues. *Phys Med Biol, 47: 163–175.*
10. Narten AH and Levy HA (1971) Liquid water: molecular correlation functions from x-ray diffraction. *J Chem Phys, 55: 2263–2269.*
11. Hubbell JH, Veigele EA, Briggs EA, Brown DT, Cromer DT, Howerton RJ (1975) Atomic form factors, incoherent scattering functions and photon scattering cross sections. *J Phys Chem Ref Data, 4: 471–538.*
12. ICRU (1989) *ICRU Report* 44 (Bethesda, MD: ICRU)
13. Johns PC and Wismayer MP (2004) Measurement of coherent X-ray scatter form factors for amorphous materials using diffractometers. *Phys Med Biol, 49: 5233–5250.*